

# We are IntechOpen, the world's leading publisher of Open Access books Built by scientists, for scientists

## 4,800

Open access books available

## 122,000

International authors and editors

## 135M

Downloads

Our authors are among the

## 154

Countries delivered to

## TOP 1%

most cited scientists

## 12.2%

Contributors from top 500 universities

**WEB OF SCIENCE™**Selection of our books indexed in the Book Citation Index  
in Web of Science™ Core Collection (BKCI)

Interested in publishing with us?  
Contact [book.department@intechopen.com](mailto:book.department@intechopen.com)

Numbers displayed above are based on latest data collected.

For more information visit [www.intechopen.com](http://www.intechopen.com)

# Time-Frequency Analysis for Rotor-Rubbing Diagnosis

Eduardo Rubio and Juan C. Jáuregui  
*CIATEQ A.C., Centro de Tecnología Avanzada  
Mexico*

## 1. Introduction

Predictive maintenance by condition monitoring is used to diagnose machinery health. Early detection of potential failures can be accomplished by periodic monitoring and analysis of vibrations. This can be used to avoid production losses or a catastrophic machinery breakdown. Predictive maintenance can monitor equipments during operation. Predictions are based on a vibration signature generated by a healthy machine. Vibrations are measured periodically and any increment in their reference levels indicates the possibility of a failure.

There are several approaches to analyze the vibrations information for machinery diagnosis. Conventional time-domain methods are based on the overall level measurement, which is a simple technique for which reference charts are available to indicate the acceptable levels of vibrations. Processing algorithms have been developed to extract some extra features in the vibrations signature of the machinery. Among these is the Fast Fourier Transforms (FFT) that offers a frequency-domain representation of a signal where the analyst can identify abnormal operation of the machinery through the peaks of the frequency spectra. Since FFT cannot detect transient signals that occur in non-stationary signals, more complex analysis methods have been developed such as the wavelet transform. These methods can detect mechanical phenomena that are transient in nature, such as a rotor rubbing the casing of a motor in the machine. This approach converts a time-domain signal into a time-frequency representation where frequency components and structured signals can be localized. Fast and efficient computational algorithms to process the information are available for these new techniques.

A number of papers can be found in the literature which report wavelets as a vibration processing technique. Wavelets are multiresolution analysis tools that are helpful in identifying defects in mechanical parts and potential failures in machinery. Multiresolution has been used to extract features of signals to be used in classifications algorithms for automated diagnosis of machine elements such as rolling bearings (Castejón et al., 2010; Xinsheng & Kenneth, 2004). These elements produce clear localized frequencies in the vibration spectrum when defects are developing. However, a more complex phenomena occurs when the rotor rubs a stationary element. The impacts produce vibrations at the fundamental rotational frequency and its harmonics, and additionally yield some high frequency components, that increase as the severity of the impacts increases (Peng et al., 2005).

Rotor dynamics may present light and severe rubbing, and both are characterized by a different induced vibration response. It is known that conditions that cause high vibration

levels are accompanied by significant dynamic nonlinearity (Adams, 2010). The resonance frequency is modified because of the stiffening effect of the rubbing on the rotor (Abuzaid et al., 2009). These systems are strongly nonlinear and techniques have been applied for parameter identification. These techniques have developed models that explain the jump phenomenon typical of partial rub (Choi, 2001; Choi, 2004).

The analysis of rubbing is accomplished with the aid of the Jeffcott rotor model for lateral shaft vibrations. This model states the idealized equations of rotor dynamics (Jeffcott, 1919). Research has been done to extend this model to include the nonlinear behavior of the rotor system for rubbing identification. It has been shown that time-frequency maps can be used to analyze multi-non-linear factors in rotors. They also reveal many complex characteristics that cannot be discovered with FFT spectra (Wang et al., 2004). Other approaches use analytical methods for calculating the nonlinear dynamic response of rotor systems. Second-order differential equations which are linear for non-contact and strongly nonlinear for contact scenarios have been used (Karpenko et al., 2002). Rub-related forces for a rotor touching an obstacle can be modeled by means of a periodic step-function that neglects the transient process (Muszynska, 2005).

In this chapter the phenomenon of rotor rubbing is analyzed by means of a vibrations analysis technique that transforms the time-domain signal into the time-frequency domain. The approach is proposed as a technique to identify rubbing from the time-frequency spectra generated for diagnostic purposes. Nonlinear systems with rotating elements are revised and a nonlinear model which includes terms for the stiffness variation is presented. The analysis of the signal is made through the wavelet transform where it is demonstrated that location and scale of transient phenomena can be identified in the time-frequency maps. The method is proposed as a fast diagnostic technique for rapid on-line identification of severe rubbing, since algorithms can be implemented in modern embedded systems with a very high computational efficiency.

## 2. Nonlinear rotor system with rubbing elements

Linear models have intrinsic limitations describing physical systems that show large vibration amplitudes. Particularly, they are unable to describe systems with variable stiffness. To reduce the complexity of nonlinear problems, models incorporate simplified assumptions, consistent with the physical situation, that reduce their complexity and allow representing them by linear expressions. Although linearized models capture the essence of the problem and give the main characteristics of the dynamics of the system, they are unable to identify instability and sudden changes. These problems are found in nonlinear systems and the linear vibration theory offers limited tools to explain the complexity of their unpredictable behavior. Therefore, nonlinear vibration theories have been developed for such systems.

The steady state response of the nonlinear vibration solution exhibits strong differences with respect to the linear approach. One of the most powerful models for the analysis of nonlinear mechanical systems is the Duffing equation. Consider the harmonically forced Duffing equation with external excitation:

$$\ddot{x} + c\dot{x} + ax + \beta x^3 = a\cos(\omega t + \phi) \quad (1)$$

Curves of response amplitude versus exciting frequency are often employed to represent this vibration behavior as shown in Fig. 1. The solid line in this figure shows the response

curve for a linear system. The vertical line at  $\omega/\omega_n=1$  corresponds to the resonance. At this point vibration amplitude increases dramatically and it is limited only by the amount of damping in the system. It is important to ensure that the system operates outside of this frequency to avoid excessive vibration that can result in damage to the mechanical parts. In linear systems amplitude of vibrations grows following a straight line as excitation force increases.

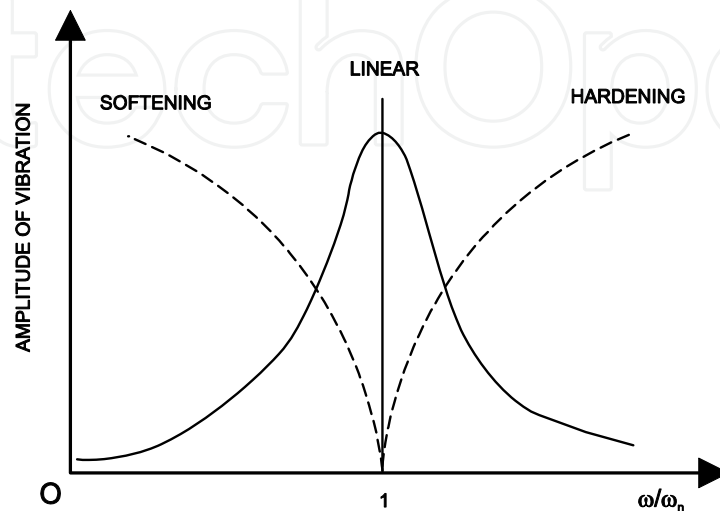


Fig. 1. Resonant frequency dependency in nonlinear systems

In nonlinear systems the motion follows a trend that is dependent upon the amplitude of the vibrations and the initial conditions. The resonance frequency is a function of the excitation force and the response curve does not follow a straight line. When the excitation force increases, the peak amplitude “bends” to the right or left, depending on whether the stiffness of the system hardens or softens. For larger amplitudes, the resonance frequency decreases with amplitude for softening systems and increases with amplitude for hardening systems. The dashed lines in Fig. 1 show this effect.

When the excitation force is such that large vibration amplitudes are present, an additional “jump” phenomenon associated with this bending arises. This is observed in Fig. 2. Jump phenomenon occurs in many mechanical systems. In those systems, if the speed is increased the amplitude will continue increasing up to values above  $1.6\omega_n$ .

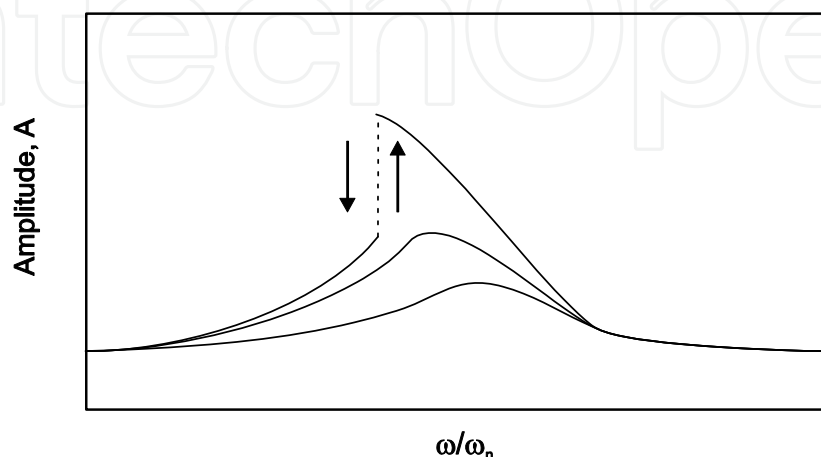


Fig. 2. Jump phenomenon typical of nonlinear systems

When the excitation force imposes low vibration amplitudes, or there is a relative strong damping, the response curve is not very different from the linear case as it can be observed in the two lower traces. However, for large vibration amplitudes the bending effect gets stronger and a “jump” phenomenon near the resonance frequency is observed. This phenomenon may be observed by gradually changing the exciting frequency  $\omega$  while keeping the other parameters fixed. Starting from a small  $\omega$  and gradually increasing the frequency, the amplitude of the vibrations will increase and follow a continuous trend. When frequency is near resonance, vibrations are so large that the system suddenly exhibits a jump in amplitude to follow the upper path, as denoted with a dashed line in Fig. 2. When reducing the excitation frequency the system will exhibit a sudden jump from the upper to the lower path. This unusual performance takes place at the point of vertical tangency of the response curve, and it requires a few cycles of vibration to establish the new steady-state conditions.

There is a region of instability in the family of response curves of a nonlinear system where such amplitudes of vibration cannot be established. This is shown in Fig. 3. It is not possible to obtain a particular amplitude in this region by forcing the exciting frequency. Even with small variations the system is unable to restore the stable conditions. Therefore, from the three regions depicted in this figure, only the upper and lower amplitudes of vibration exist. The same applies for a hardening system but with the peaks of amplitude of vibrations bending to the right.

A rotor system with rub impact is complex and behaves in a strong nonlinearity. A complicated vibration phenomenon is observed and the response of the system may be characterized by the jump phenomena at some frequencies. Impacts are associated with stiffening effects; therefore, modeling of rotor rub usually includes the nonlinear term of stiffness.

When the rotor hits a stationary element, it involves several physical phenomena, such as stiffness variation, friction, and thermal effects. This contact produces a behavior that worsens the operation of the machine. Rubbing is a secondary transient phenomenon that arises as a result of strong rotor vibrations. The transient and chaotic behavior of the rotor impacts generate a wide frequency bandwidth in the vibrational response.

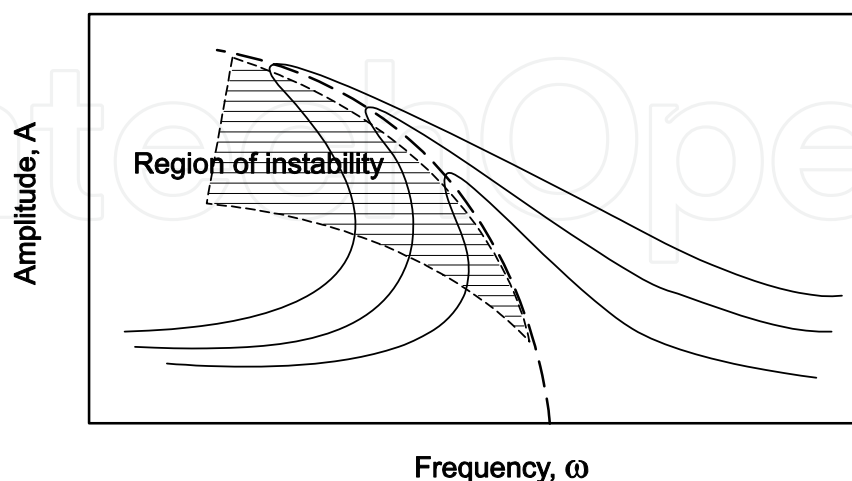


Fig. 3. Region of instability

Dynamics of the rotor rubbing can be studied with the Jeffcott rotor model (Jeffcott, 1919). This model was developed to analyze lateral vibrations of rotors and consists of a centrally

mounted disk on a flexible shaft. Rigid bearings support the ends of the shaft as shown in Fig. 4. The model is more representative of real rotor dynamics for the inclusion of a damping force proportional to the velocity of the lateral motion. The purpose of this model was to analyze the effect of unbalance at speeds near the natural frequency, since the vibration amplitude increase considerably in this region.

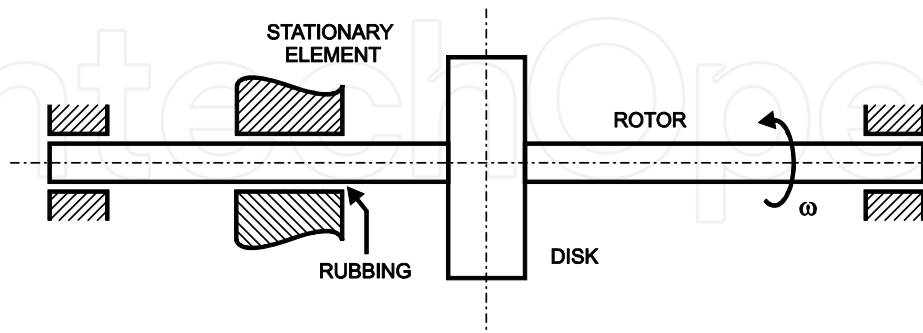


Fig. 4. Diagram of a rotor rubbing with a stationary element

Modifying the Jeffcott's model, the rubbing phenomenon can be studied. A stationary element can be added to the model to take rubbing into consideration. A diagram of the forces that are involved during the rub-impact phenomenon is shown in Fig. 5.

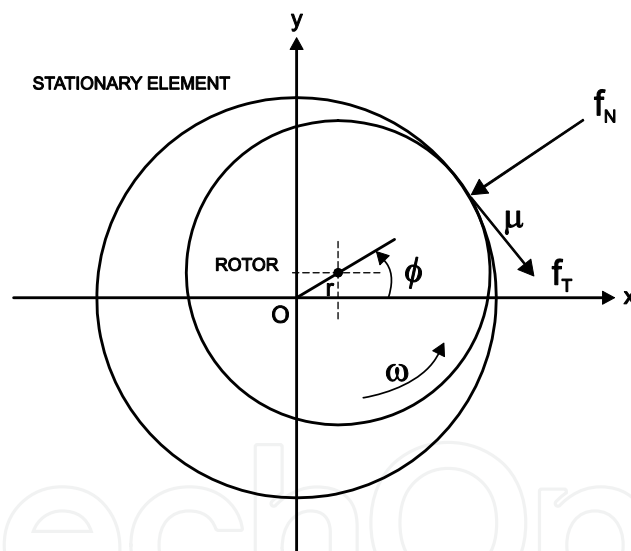


Fig. 5. A Jeffcott rotor model with rubbing

At the contact point, normal and tangential forces are described by the following expressions:

$$f_N = K_R(R - c) \quad (2)$$

$$f_T = \mu f_N \quad (3)$$

Where  $K_R$  is the combined stiffness of the shaft and the contact stiffness. This is valid for

$$R \geq c \quad (4)$$

otherwise

$$f_N = f_T = 0 \quad (5)$$

For a Cartesian coordinate system forces are represented as:

$$f_x = -f_N \cos \phi + f_T \sin \phi \quad (6)$$

$$f_y = -f_N \sin \phi - f_T \cos \phi \quad (7)$$

And the motion equations of the rotor system are described by:

$$M\ddot{x} + C\dot{x} + K(\omega)x = F_x + m\rho\omega^2 \cos(\varphi_0 + \omega t) \quad (8)$$

$$M\ddot{y} + C\dot{y} + K(\omega)y = F_y + MP\omega^2 \sin(\varphi_0 + \omega t) \quad (9)$$

Where  $K$  is the stiffness of the system and  $C$  is the damping coefficient of the system.

The contact of the rotor with the stationary element creates a coupling of the system that causes a variation in the stiffness because of the non-continuous  $f_N$  and the model becomes nonlinear. The rotor rubs the element only a fraction of the circumferential movement and the stiffness value varies with respect to the rotor angular position.

The nonlinear behavior can be related to the stiffness variation. As shown in Fig. 6, the system's stiffness can be related to the shaft stiffness  $K_s$ , and it increases to  $K_R$  during contact. This increment can be estimated using the Hertz theory of contact between two elastic bodies placed in mutual contact.

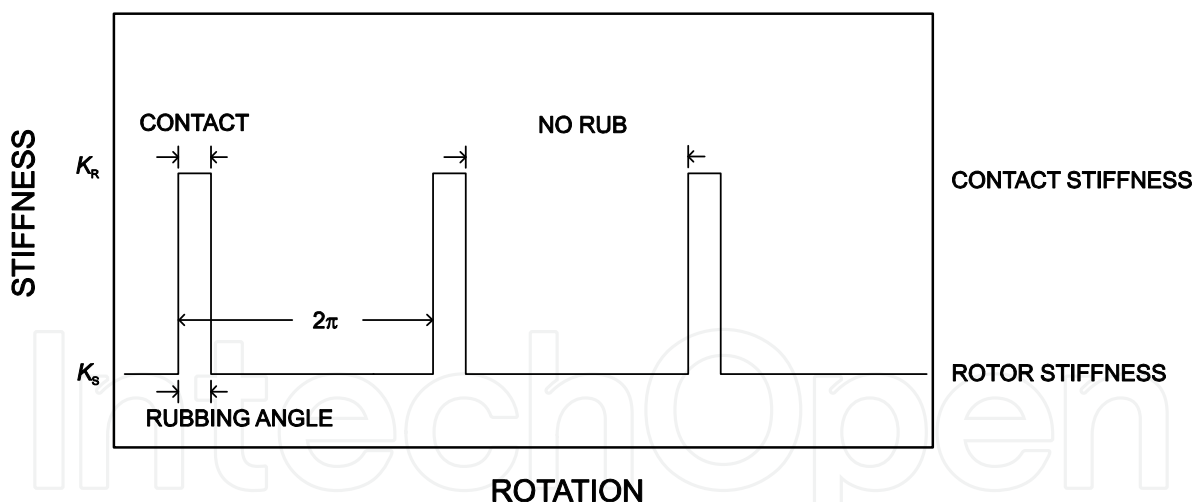


Fig. 6. Stiffness increase during contact

Assuming that the system's stiffness can be represented as a rectangular function, then the stiffness variation can be approximated as a Taylor series such that

$$K(\omega) = \alpha + \beta^3 \omega \quad (10)$$

### 3. Vibrations analysis with data-domain transformations

The vibrational motion produced by a rotating machine is complicated and may be analyzed by transforming data from the time-domain to the frequency-domain by means of the



Fourier Transform. This transform gives to the operator additional information from the behavior of the machine that a signal in time-domain cannot offer.

Fourier developed a theory in which any periodic function  $f(t)$ , with period  $T$ , can be expressed as an infinite series of sine and cosine functions of the form:

$$f(t) = \frac{a_0}{2} + \sum_{n=1}^{\infty} (a_n \cos n\omega_T t + b_n \sin \omega_T t) \quad (11)$$

Where  $\omega$  denotes the fundamental frequency and  $2\omega$ ,  $3\omega$ , etc., its harmonics. This series is known as the Fourier series expansion and  $a_n$  and  $b_n$  are called the Fourier coefficients. By this way, a periodic waveform can be expanded into individual terms that represent the various frequency components that make up the signal. These frequency components are integer multiples of  $\omega$ .

The following identity can be used to extend the Fourier series to complex functions:

$$e^{ix} = \cos(x) + i\sin(x) \quad (12)$$

$$f(t) = \sum_{-\infty}^{\infty} c_n e^{int} \quad (13)$$

Where  $c_n$  can be obtained by the following integration:

$$c_n = \frac{1}{2\pi} \int_{-\pi}^{\pi} f(t) e^{-int} dt \quad (14)$$

This applies to periodic functions on a  $2\pi$  interval.

Fourier series can be extended to functions with any period  $T$  with angular frequency  $\omega=2\pi/T$ . Sine and cosine functions have frequencies that are multiples of  $\omega$  as in Eq. (11).

For non-periodic functions, with period  $T$ , discrete frequencies  $n\omega$  separated by  $\Delta\omega=2\pi/T$ , and taking the limit as  $T \rightarrow \infty$ ,  $n\Delta\omega$  becomes continuous and the summation can be expressed as an integral. As a result, the continuous Fourier transform for frequency domain is defined as:

$$F(\omega) = \int_{-\infty}^{+\infty} f(t) e^{-i\omega t} dt \quad (15)$$

While for time domain the inverse Fourier transform is defined as:

$$f(t) = \frac{1}{2\pi} \int_{-\infty}^{+\infty} F(\omega) e^{i\omega t} d\omega \quad (16)$$

And  $f=f(t)$  satisfying the condition

$$\int_{-\infty}^{+\infty} |f(t)|^2 dt < \infty \quad (17)$$

Since computers can't work with continuous signals, the Discrete Fourier Transform (DFT) was developed and implemented through the Fast Fourier Transform (FFT). The FFT is a fast algorithm for computing the DFT that requires the size of the input data to be a power



of 2. FFT is a helpful engineering tool to obtain the frequency components from stationary signals. However, non-stationary phenomena can be present in signals obtained from real engineering applications, and are characterized by features that vary with time.

A difficulty that has been observed with FFT is that the complex exponentials used as the basis functions have infinite extent. Therefore, localized information is spread out over the whole spectrum of the signal. A different approach is required for this type of signals. Time-frequency methods are used for their analysis and one of the most used methods is the Short Time Fourier Transform (STFT). This was the first time-frequency technique developed. The solution approach introduces windowed complex sinusoids as the basis functions.

The STFT is a technique that cuts out a signal in short time intervals, which can be assumed to be locally stationary, and performs the conventional Fourier Transform to each interval. In this approach a signal  $S_t(\omega)$  is multiplied by a window function  $h(\tau)$ , centered at  $\tau$ , to obtain a modified signal that emphasises the signal characteristics around  $\tau$ :

$$S_t(\omega) = \frac{1}{2\pi} \int_{-\infty}^{\infty} e^{-j\omega t} s(\tau) h(\tau - t) d\tau \quad (18)$$

Frequency distribution will be reflected around  $\tau$  after applying the Fourier Transform to this window. The spectral density of the energy at time  $\tau$  can be written as follows:

$$P(t, \omega) = |S_t(\omega)|^2 = \left| \frac{1}{2\pi} \int_{-\infty}^{\infty} e^{-j\omega \tau} s(\tau) h(t - \tau) d\tau \right|^2 \quad (19)$$

As expected, a different spectrum will be obtained for each time. A Spectrogram, which is the time-frequency distribution, can be constructed with the resulting spectra. Resolution in time and frequency depends on the width of the windows  $h(\tau)$ . Large windows will provide a good resolution in the frequency domain, but poor resolution in time domain. Small windows will provide good resolution in time domain, but poor resolution in frequency domain. The major disadvantage of this approach is that resolution in STFT is fixed for the entire time-frequency map. This means that a single window is used for all the frequency analysis. Therefore, only the signals that are well correlated in the time interval and frequency interval chosen will be localized by the procedure. It may be thought of as a technique to map a time-domain signal into a fixed resolution time-frequency domain.

This drawback can be surpassed with basis functions that are short enough to localize high frequency discontinuities in the signal, while long ones are used to obtain low frequency information. A new transform called wavelet transform achieves this with a single prototype function that is translated and dilated to get the required basis functions.

The wavelet transform is a time-frequency representation technique with flexible time and frequency resolution. Conversely to the STFT where the length of the windows function remains constant during the analysis, in the wavelet approach a function called the mother wavelet is operated by translation and dilation to build a family of window functions of variable length:

$$\psi_{s\tau}(t) = \frac{1}{\sqrt{s}} \psi\left(\frac{t - \tau}{s}\right) \quad (20)$$

Where  $\psi(t)$  is the mother wavelet function,  $s$  the scale parameter, and  $\tau$  the time shift or dilation parameter. Based on the mother wavelet function, the wavelet transform is defined as:

$$W_{\psi}x(s, \tau) = \int_{-\infty}^{\infty} x(t) \overline{\psi_{s\tau}}(t) dt \quad (21)$$

And  $W_{\psi}x(s, \tau)$  are the wavelet coefficients.

The wavelet transform is different from other techniques in that it is a multiresolution signal analysis technique that decomposes a signal in multiple frequency bands. By operating over  $s$  and  $\tau$  the wavelets permit to detect singularities, which makes it an important technique for nonstationary signal analysis.

Due to this characteristic, the wavelet transform is the analysis technique that we found more suitable for the analysis of the rubbing phenomenon.

#### 4. Experimental methodology

An experimental test rig was implemented to get a deeper understanding of the main characteristics of the rubbing phenomenon, and to apply the wavelet analysis technique in the processing and identification of the vibrations produced by the rub-impact of the system. Elements were included to run experiments under controlled conditions. Fig. 7 shows the experimental set-up.

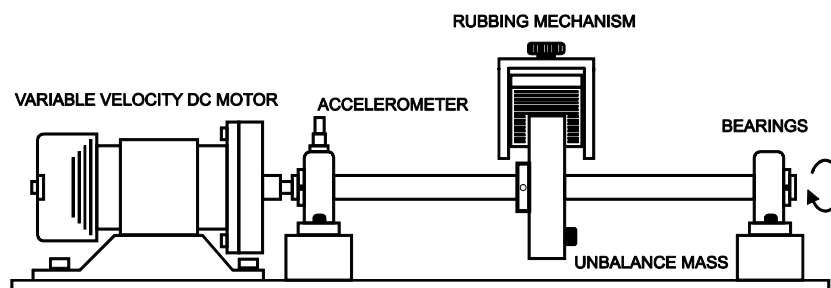


Fig. 7. Test rig for the rubbing experiments

The experimental system is composed of a shaft supported by ball bearings and coupled to an electrical motor with variable rotational speed. The velocity of the motor was controlled with an electronic circuit. A disk was installed in the middle of the shaft, which was drilled to be able to mount bolts of different masses to simulate unbalance forces. An adjustable mechanism was designed in order to simulate the effect of a rotor rubbing a stationary element. The position of the device, acting as the stationary element, was adjusted with a threaded bolt that slides a surface to set the clearance between the rotating disk and the rubbing surface. The shaft and disk were made of steel, and the rubbing device of aluminium alloy. Light and severe rubbing were simulated by controlling the speed of the rotor. Low velocities caused light rubbing while high velocities generated severe impact-like rubbing vibrations. Both types of rubbing were analyzed with the proposed methodology.

An accelerometer was used to measure the vibrations amplitude. Output of the accelerometer was connected to a data acquisition system to convert analog signals to digital data with a sampling rate of 10 kHz. An antialias filter stage was included to get a band limited input signal.

Experimental runs were carried out for fixed and variable rotor velocities. Fixed velocities were tested for values between 350 rpm and 1900 rpm. Continuous variable velocity experiments were also carried out to simulate a rotor system under ramp-up and ramp-down conditions, to verify the preservation of the scale and temporal information with the processing technique used.

Daubechies 4 wavelet transform was implemented to convert the signal from the time-domain to the time-frequency domain. Scaling and wavelet functions for this transform are shown in Fig. 8.

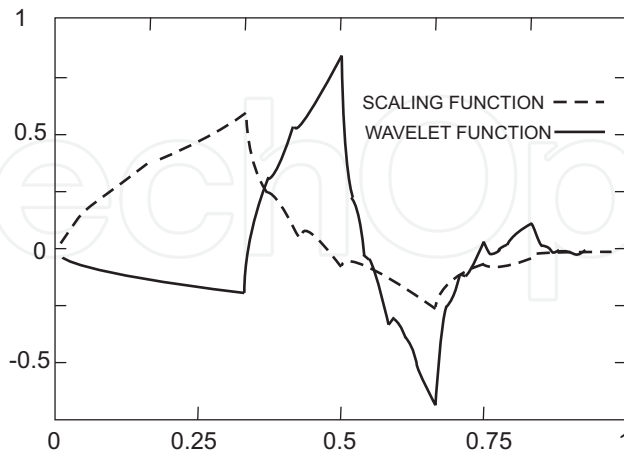


Fig. 8. Daubechies D4 scaling and wavelet functions

Implementation of the continuous wavelet transform is impractical, especially for on-line detection devices for process monitoring purposes. This implementation consumes a significant amount of time and resources. An algorithm for the discrete wavelet transform (DWT) is used to overcome this situation. It is based on a sub-band coding which can be programmed with a high computational efficiency. Subband coding is a multiresolution signal processing technique that decomposes the signal into independent frequency subbands.

With this approach, the DWT applies successive low-pass and high-pass filters to the discrete time-domain signal as shown in Fig. 9. This procedure is known as the Mallat algorithm.

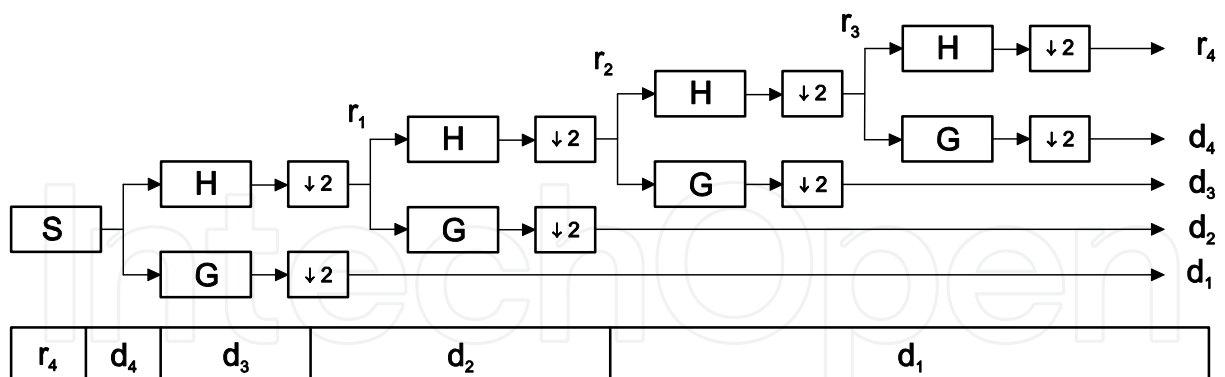


Fig. 9. Algorithm for the sub-band decomposition of the input signal

The algorithm uses a cascade of filters to decompose the signal. Each resolution has its own pair of filters. A low-pass filter is associated with the scaling function, giving the overall picture of the signal or low frequency content, and the high-pass filter is associated with the wavelet function, extracting the high frequency components or details. In Fig. 9 the low-pass filter is denoted by H and the high-pass filter is denoted by G. Each end row is a level of decomposition. A sub-sampling stage is added to modify the resolution by two at each step of the procedure. As a result of this process, time resolution is good at high frequencies, while frequency resolution is good at low frequencies.

For each transform iteration the scale function to the input data is applied through the low-pass and high-pass filters. If the input array has  $N$  cells, after applying the scale function, the down-sampling by two, which follows the filtering, halves the resolution and an array with  $N/2$  values will be obtained. With the low-pass branch, coarse approximations are obtained. The high-pass filtered signal will reflect the fluctuations or details content of the signal. By iterating recursively a signal is decomposed into sequences. The successive sequences are lower resolution versions of the original data.

The implemented form of the Daubechies 4 wavelet transform has a wavelet function with four coefficients and a scale function with four coefficients. The scale function is:

$$A_i = H_0 S_{2i} + H_1 S_{2i+1} + H_2 S_{2i+2} + H_3 S_{2i+3} \quad (22)$$

Where scaling coefficients are defined as

$$H_0 = \frac{1 + \sqrt{3}}{4\sqrt{2}} \quad (23)$$

$$H_1 = \frac{3 + \sqrt{3}}{4\sqrt{2}} \quad (24)$$

$$H_2 = \frac{3 - \sqrt{3}}{4\sqrt{2}} \quad (25)$$

$$H_3 = \frac{1 - \sqrt{3}}{4\sqrt{2}} \quad (26)$$

The wavelet function is:

$$C_i = G_0 S_{2i} + G_1 S_{2i+1} + G_2 S_{2i+2} + G_3 S_{2i+3} \quad (27)$$

Where wavelet coefficients are defined as

$$G_0 = H_3 \quad (28)$$

$$G_1 = -H_2 \quad (29)$$

$$G_2 = H_1 \quad (30)$$

$$G_3 = -H_0 \quad (31)$$

Each wavelet and function value is calculated by taking the product of the coefficients with four data values of the input data array. The process is iterated until desired results are reached.

## 5. Experimental results and discussion

The methodology described in the previous section was applied and experimental runs were carried out with the aid of the test rig to obtain a deeper comprehension of the rubbing phenomenon. Fig. 10 shows results for time and frequency domains for the rotor rubbing

and no-rub experimental runs. The upper row corresponds to time-domain signals, while the lower row shows the frequency-domain signals.

With no-rub (upper left), the signal in time-domain is characterized by a uniform trace with a small dispersion of data produced by the low-level noise of the measuring system. However, when rub occurs (upper right), as acceleration is the measurement engineering unit, even for low level rubbing the energy content of the signal is high, and spikes appear at the location of each rub-contact.

The spectral distribution of the signal obtained when the rotor is rubbing shows the wide frequency bandwidth in the vibrational response, produced by the chaotic behavior of the rubbing phenomenon.

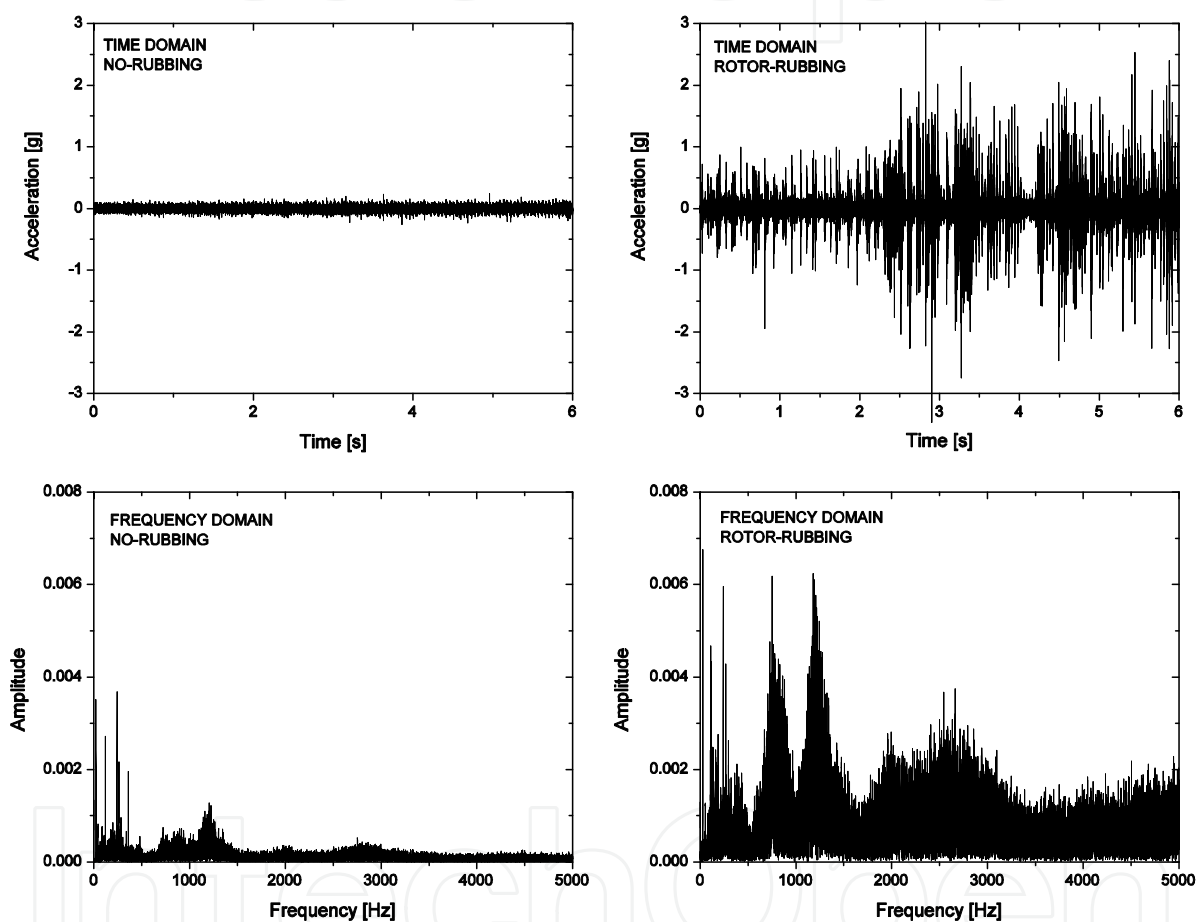


Fig. 10. Spectral distribution of the vibrations for the rotor rubbing and no-rubbing

When rubbing is present, the response is dependent on the angular frequency of the rotor. For low rotor velocities rub generates low vibration amplitudes as shown in the acceleration values in the upper graph of Fig. 11. This can be considered a light-rubbing, but when the rotor velocity is high, the time-domain response of the vibrations produced is quite different and get closer to an impact response characterized by spikes with high acceleration values. This response can be seen in the lower graph of Fig. 11. The amplitudes of vibrations for light rubbing are within  $\pm 0.1$  g, while for severe rubbing peak values reach  $\pm 1$  g, about ten times higher.

Processing results of the signals for the rotor with rubbing and without rubbing to obtain the spectral distribution are shown in Fig. 12. The graph localizes the natural frequency of

the test rig for both cases. As explained in the introductory section, the nonlinear nature of the system produced a slight different vibrations pattern when rubbing is present. Solid line shows the natural frequency for the rub-free experiments. However, the dotted line corresponds to the experiments with rubbing induced to the rotor, and as expected there is a shift in the natural frequency.

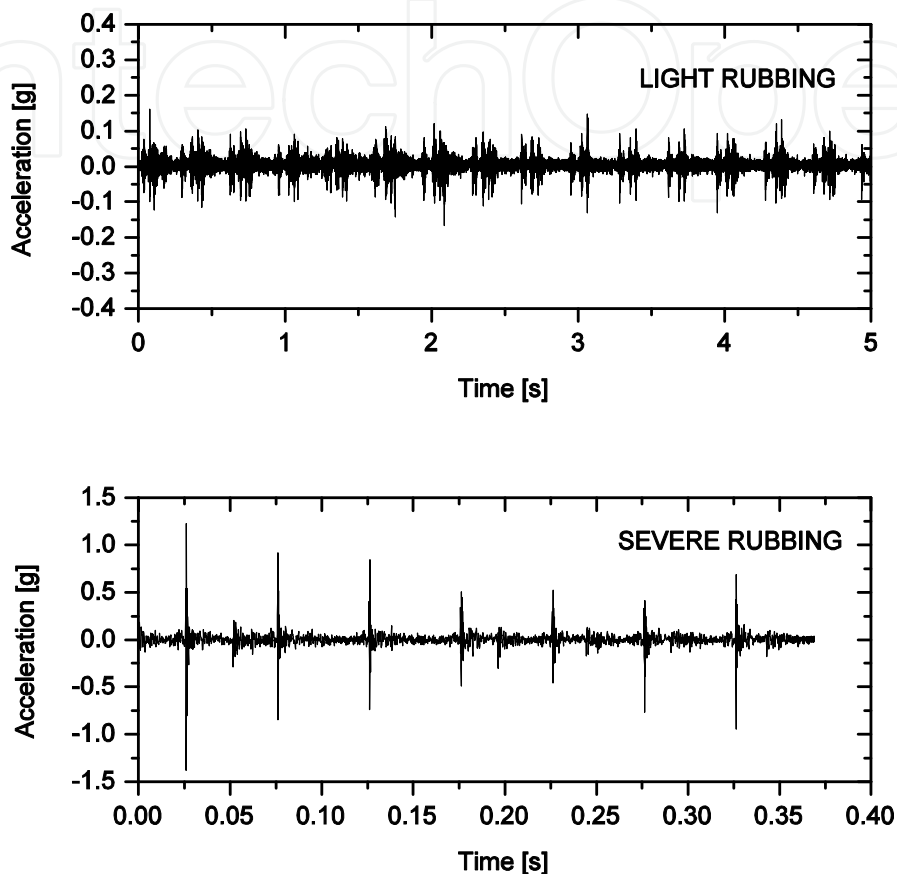


Fig. 11. Vibrations amplitude for light rubbing and severe rubbing

Frequency shift occurs to the right, with the trend to move to the high frequency side of the spectrum, which means that the system is hardening as a result of the stiffness increase produced by the contact of the rotor with the stationary element. The amplitude of the natural frequency also increases as a product of the higher energy content of the rub-impacts.

The signal of the vibrations was processed to transform the data from the time-domain to the time-frequency domain. Wavelet transform Daubechies 4 was used for the transformation and results are shown in Fig. 13.

As stated before, a vector is obtained with this procedure which is the same size as the original vector. Recalling the subband coding, upper half of the vector contains the high frequency content of the information (subband 1). From the remaining data, upper half contains the next subband with mid-frequency content (subband 2), and so on. This way, the low frequency content of the information is coded and located in the lower part of the vector while the high frequency content is coded into the higher indexes of the vector. Indexes



represent the transformed values in the resulting vector which amplitude is a function of the correlation between the input signal and the mother wavelet. A higher value for the index means a stronger correlation and therefore a major content of that frequency corresponding to a particular value of scale and translation.

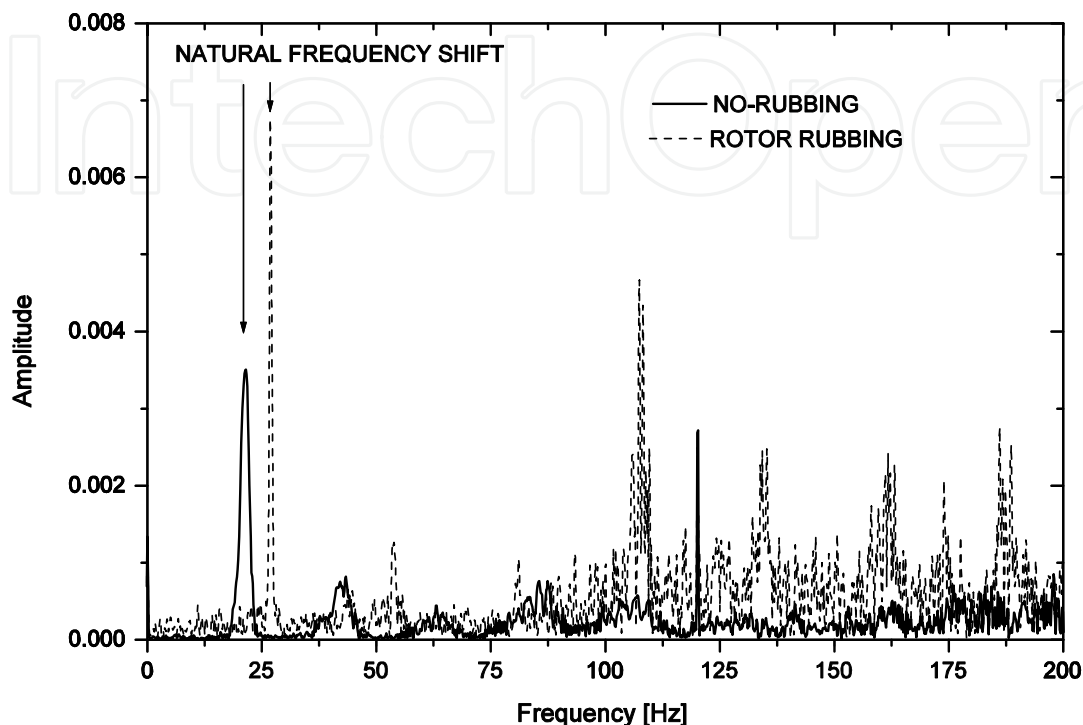


Fig. 12. Resonance frequency dependence observed for a rotor with rubbing

Taking this into consideration, it can be observed that for light rubbing the correlation gets stronger for mid-value indexes, which means that light rubbing is characterized by frequencies that fall in the lower middle of the frequency spectrum.

On the other side, rub-impacts produced by the contact of the rotor with the stationary element at high rotational frequencies, are characterized by spikes with a high frequency content. The wavelet transformation enhances this type of rubbing as can be observed in the upper half of the vector for severe rubbing shown in Fig. 13 (subband 1), although some rubbing information can be found in the next subband. As both light and severe rubbing may be present in a rotor, the sum of the frequency content produced by the phenomena reflects again a wide spectral distribution in the vibrational response.

To test the wavelet approach as a rubbing detection technique, especially for severe rubbing where it is desirable to assess alert signals before a catastrophic failure occurs as it can happen under some rubbing conditions, a vibration signal which presents rub-impacts was chosen. The test data are shown in Fig. 14.

There are two spikes in the graph produced by the rotor rubbing at high velocity rotation. These spikes can be treated as singularities of transient nature whose occurrence cannot be predicted. A technique like wavelets that analyzes a signal by comparison of a basis wavelet that is scaled and translated to extract frequency and location information is ideal for this situation. The procedure enhances these singularities and makes it easier their detection as it is demonstrated next.



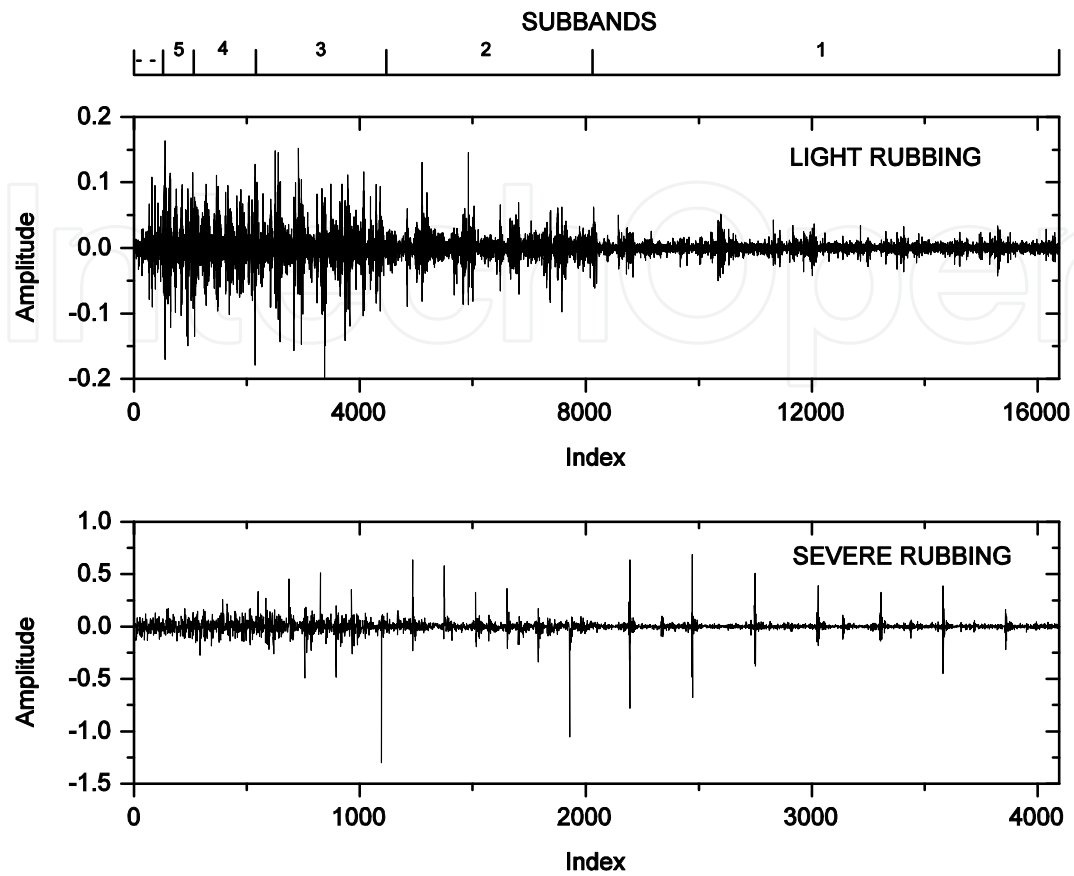


Fig. 13. Rotor rubbing signal transformed to time-frequency domain with wavelets

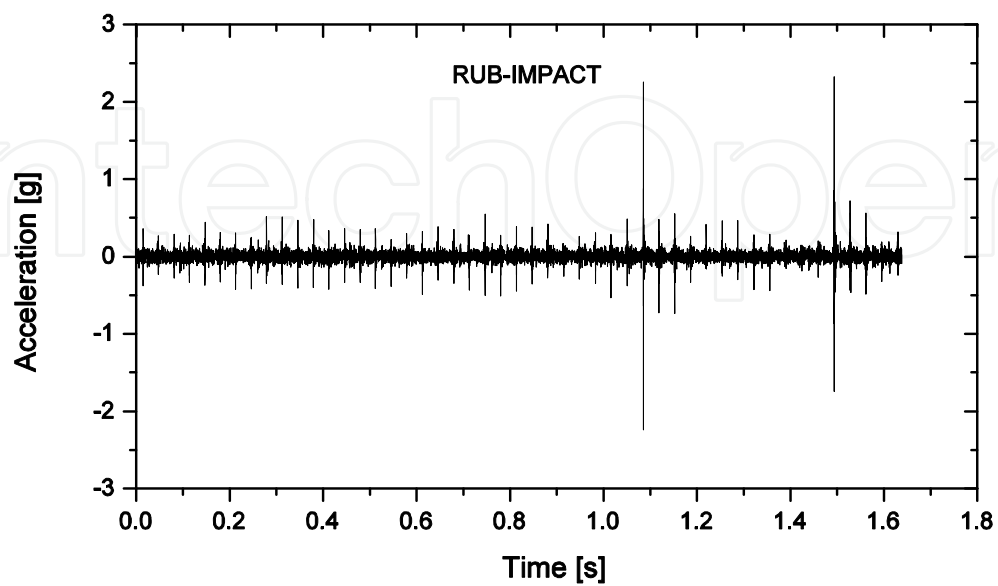


Fig. 14. Time-domain vibrations with rub-impact

Graphs showing the details of the impacts are shown in Fig. 15. The signal is characterized by a sudden excitation that generates a mechanical oscillation that grows to peak amplitude and decays as the impact energy dissipates. Each impact is characterized by only a few cycles that analyzed with the traditional FFT would not have enough energy to obtain a clear spectral definition.

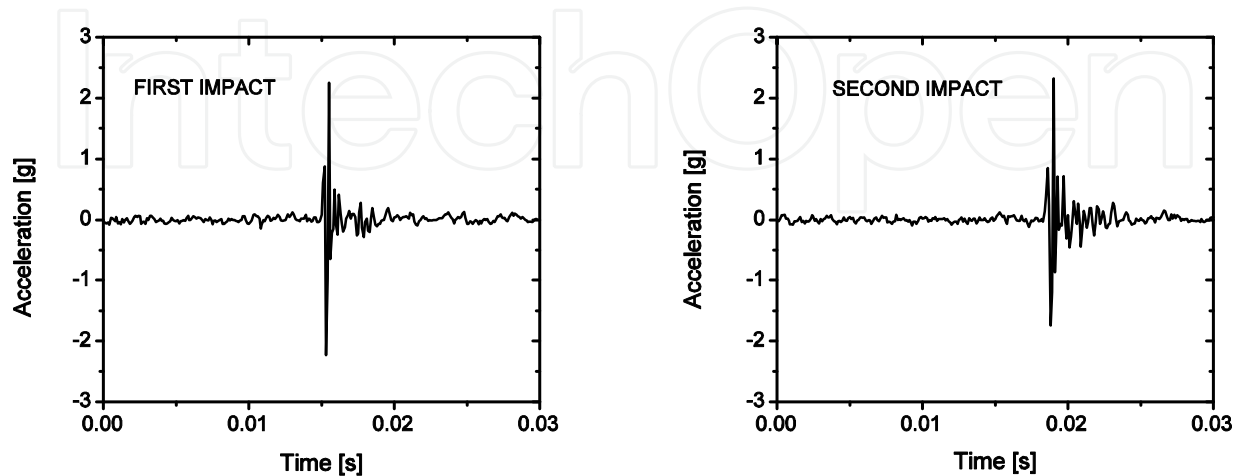


Fig. 15. Details of the transient impacts analyzed

A wavelet decomposition of this signal was made and the main subbands are shown in Fig. 16. Subbands are associated with their corresponding frequency range according to the sampling rate established during the experiments. The graph shows the frequency content between 78 Hz and 5 kHz.

From this graph it is observed that the subband with the higher frequency content encompasses the information of the transient signals. The correlation technique enhances the spikes giving amplitude values higher than the coefficients where impacts are not present. This makes it easier to establish a discrimination criterion and an estimation of their values to determine the presence and severity of the rubbing for diagnostic purposes. Additionally, as the transient signals produced are in the first subband, only the first level of decomposition in the wavelet transformation is necessary reducing the computing time that it takes to make the analysis and optimizing the detection process.

The experimental results of the vibrations presented in the previous discussion were analyzed through one of the approaches that wavelets offer to the vibration analyst. This is a time-frequency representation of the data from which it can be extracted the information of interest to apply the necessary processes and criteria for the rubbing detection. This approach permits the characterization of the signal from which it can be obtained the necessary information for the implementation of the technique for the design of testing equipment with automatic detection and recognition of the rubbing phenomena.

Another type of representation of the information that wavelets offer are the time-frequency maps. These are contour plots where the wavelet coefficient values are plotted against the time and scale parameter, that is, translation and frequency. One axis represents time, the other axis frequency, and the amplitude of the vibrations is color-coded. The contour maps permit to visualize the whole picture of the frequencies present in the signal as well as their occurrence or location in time.

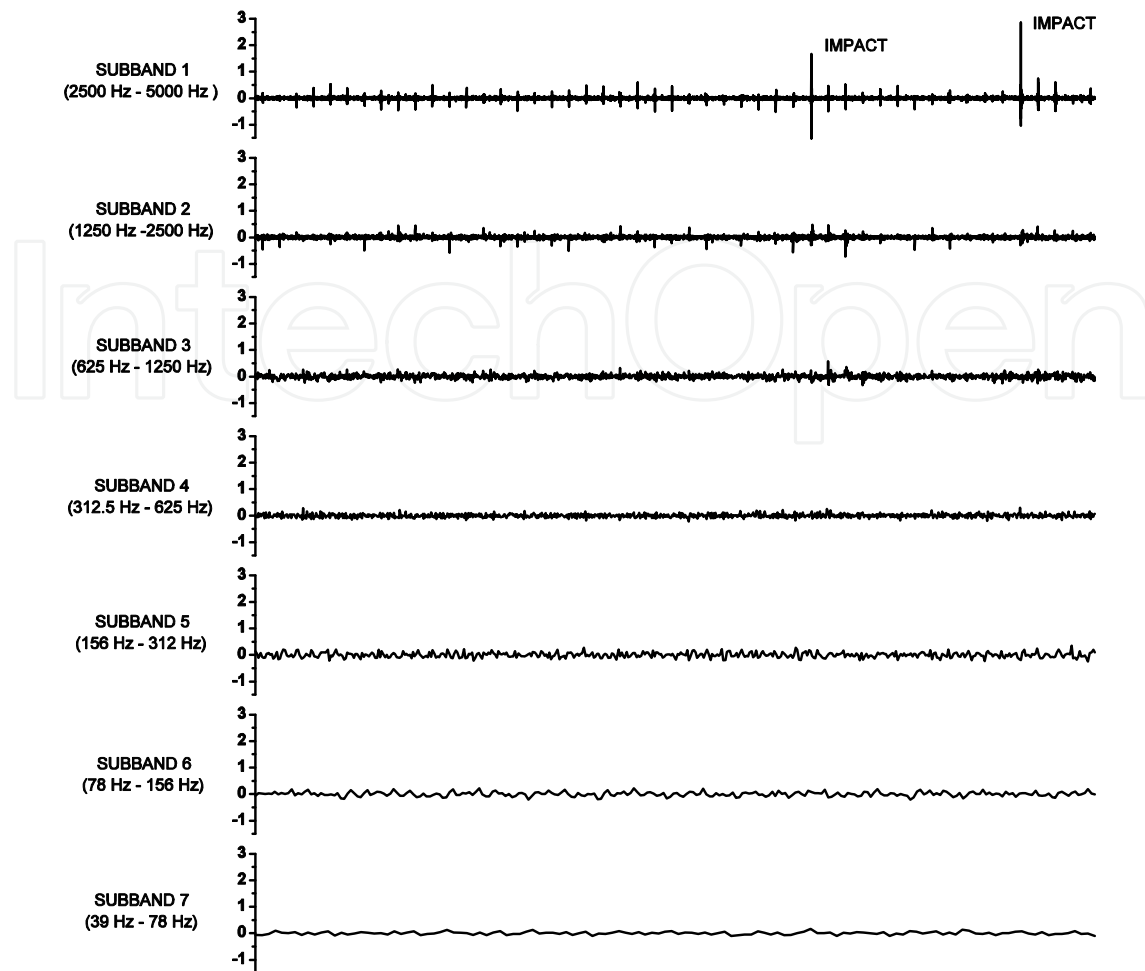


Fig. 16. Subband coding with wavelets of the vibrational response with impact-rubbing

The light rubbing data was processed with commercially available software by means of the Morlet continuous wavelet transform and results are shown in Fig. 17. In this graph, the color coding is red for low amplitude vibrations throughout blue for high amplitude vibrations. It can be observed the intermittent nature of the rubbing and, in concordance with Fig. 13, that the main vibrations are limited to frequencies below 1 250 Hz.

An analogous process was applied to severe rubbing data and results are shown in Fig. 18. The image shows that mid-range frequencies get stronger while high frequencies appear as a result of the increase in the vibrations amplitude as in the lower graph of Fig. 13. Upper spots in the time-frequency map (rub-impacts) appear elongated and lower spots stretched due to the compromise between the time and frequency resolution of the technique as stated in the introduction.

Additionally, an experimental run was carried out varying continuously the rotating conditions to obtain a sweep from a low to a high velocity and then decreasing the velocity until a minimum value. Results are shown in Fig. 19.

It can be seen that as time runs throughout the experiment, velocity increases and higher frequency components appear. These components get their peak value near the middle of the time axis where the maximum velocity is reached, and then begin to fade showing the trend of the higher frequencies to disappear as velocity decreases. This graph confirms the wide spectral bandwidth of the rubbing phenomena.

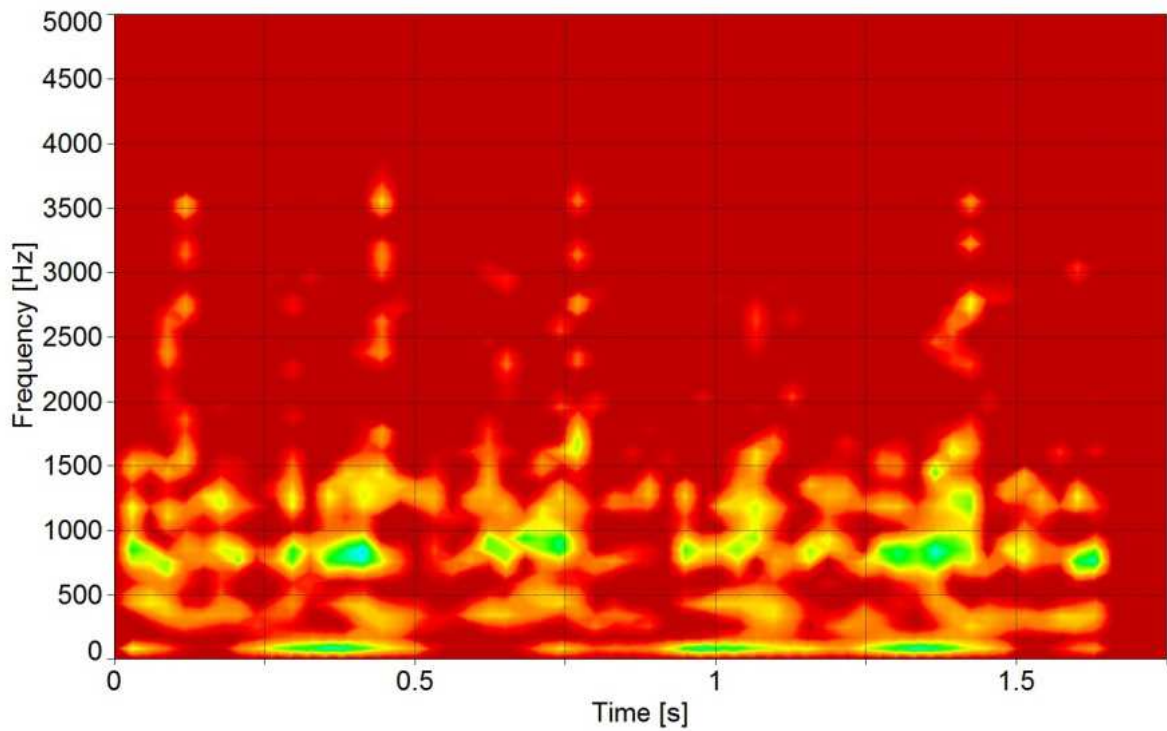


Fig. 17. Time-Frequency map for light rubbing

It is important to notice the evolution of the frequencies as time passes by. There is an unsteady variation of frequencies, and in Fig. 19 it can be seen how they have an unsymmetrical pattern even with speed variations.

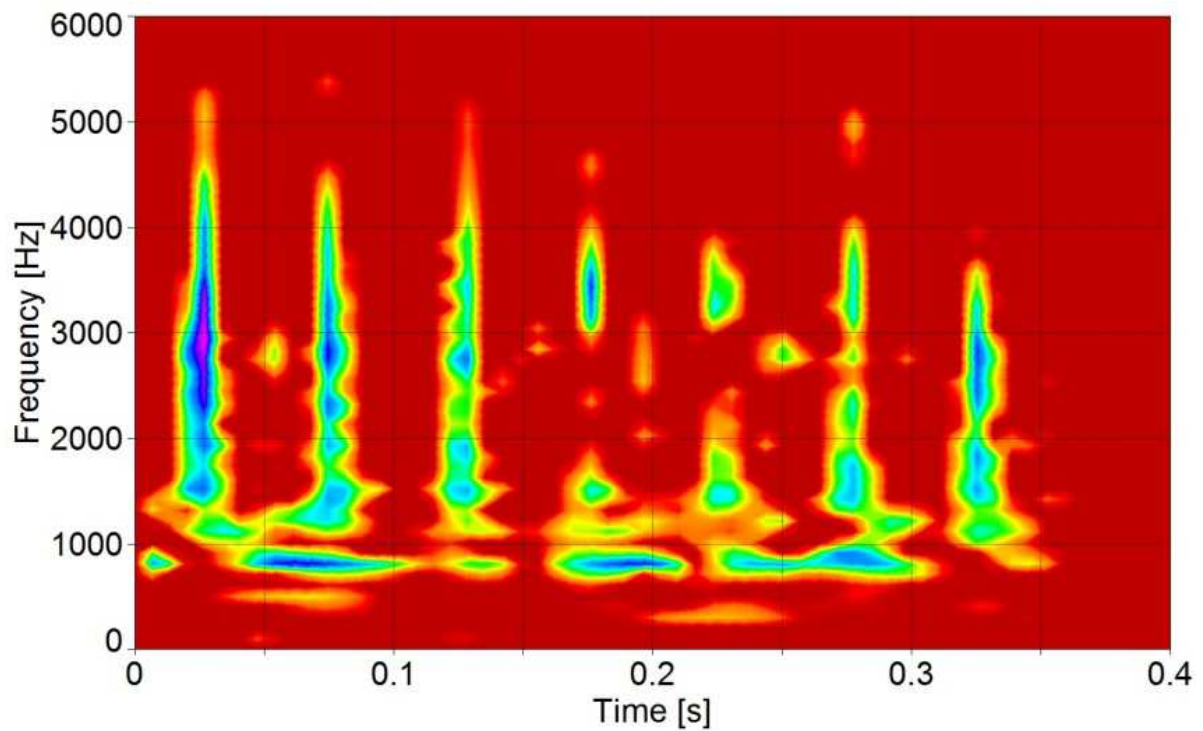


Fig. 18. Time-frequency map for severe rubbing

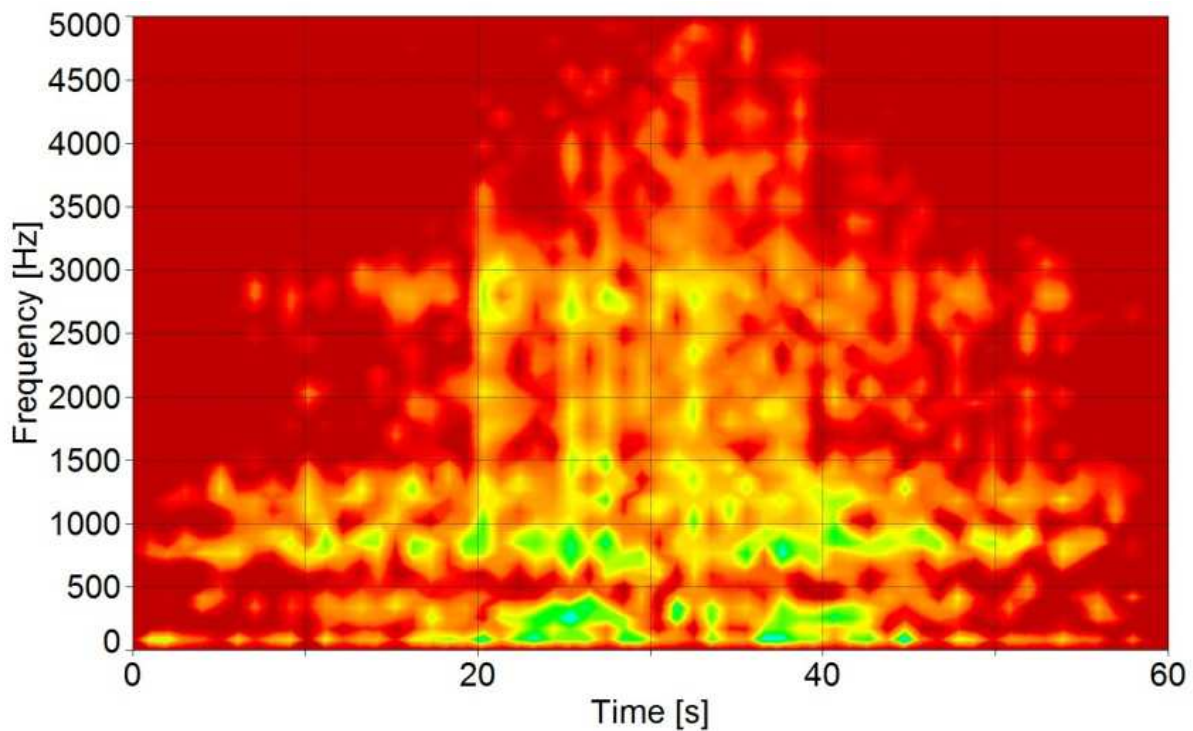


Fig. 19. Time-frequency map for a run-up and run-down rotor velocity sweep

## 6. Conclusions

Rotor rubbing has been analyzed with a methodology that processes the vibrations signal in such a way that time and scale information is preserved. It was demonstrated that with this approach vibrations of transient nature can be studied through a controlled subband coding scheme and time-frequency spectra. The technique revealed additional information that traditional processing techniques cannot, such as FFT. Experimental results showed that light rubbing presents a vibrational response characterized by a rich frequency content spectrum, and that severe rubbing is more adequately described as an impact-like transient behavior. Accordingly, impacts could be identified and localized with wavelets in the upper-frequency subbands which resulted after the algorithm was applied.

Since rotor-to-stator contact changes the effective stiffness of the coupled elements, a frequency shift was identified that shows the nonlinear response of the system. Time-frequency maps evidenced again the wide spectral response and differences between light and severe rotor rubbing, and location in time of the rub-impacts. The processing algorithm can be implemented with a high computational efficiency for on-line inspection systems for continuous machinery condition monitoring.

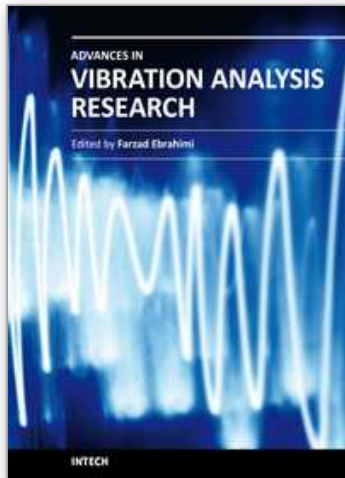
## 7. References

- Abuzaid, M.A. ; Eleshaky, M.E. & Zedan, M.G. (2009). Effect of partial rotor-to-stator rub on shaft vibration. *Journal of Mechanical Science and Technology*, Vol. 23, No. 1, 170-182.
- Adams, M.L. (2010). *Rotating Machinery Vibration*, 84, CRC Press, Taylor & Francis Group, ISBN 978-1-4398-0717-0, Boca Raton, FL, USA.



- Castejón, B; Lara, O. & García-Prada, J.C. (2010). Automated diagnosis of rolling bearings using MRA and neural networks. *Mechanical Systems and Signal Processing*, Vol. 24, No. 1, 289-299.
- Choi, Y.-S. (2001). On the contact of partial rotor rub with experimental observations. *KSME International Journal*, Vol. 15, No. 12, 1630-1638.
- Choi, Y.-S. (2004). Nonlinear parameter identification of partial rotor rub based on experiment. *KSME International Journal*, Vol. 18, No. 11, 1969-1977.
- Jeffcott, H.H. (1919). The lateral vibration of loaded shafts in the neighborhood of a whirling speed-the effects of want of balance. *Philosophical Magazine, Series 6*, Vol. 37, 304-314.
- Karpenko, E.V. ; Wiercigroch, M. ; Pavlovskaia, E.E. & Cartmell, M.P. (2002). Piecewise approximate analytical solutions for a Jeffcott rotor with a snubber ring. *International Journal of Machine Sciences*, Vol. 44, No. 3, 475-488.
- Muszynska, A. (2005). *Rotordynamics*, 646-648, CRC Press, Taylor & Francis Group, ISBN 978-0-8247-2399-6, Boca Raton, FL, USA.
- Peng, Z.K. ; Chu, F.L. & Tse, P.W. (2005). Detection of rubbing-caused impacts for rotor-stator fault diagnosis using reasigned scalogram. *Mechanical Systems and Signal Processing*, Vol. 19, No. 2, 391-409.
- Xinsheng, L. & Kenneth, A.L. (2004). Bearing fault diagnosis based on wavelet transform and fuzzy inference. *Mechanical Systems and Signal Processing*, Vol. 18, No. 5, 1077-1095.
- Wang, F. ; Xu, Q. & Li, S. (2004). Vibration analysis of cracked rotor sliding bearing systems with rotor-stator rubbing by harmonic wavelet transform. *Journal of Sound and Vibration*, Vol. 271, No. 3-5, 507-518.

IntechOpen



## **Advances in Vibration Analysis Research**

Edited by Dr. Farzad Ebrahimi

ISBN 978-953-307-209-8

Hard cover, 456 pages

**Publisher** InTech

**Published online** 04, April, 2011

**Published in print edition** April, 2011

Vibrations are extremely important in all areas of human activities, for all sciences, technologies and industrial applications. Sometimes these Vibrations are useful but other times they are undesirable. In any case, understanding and analysis of vibrations are crucial. This book reports on the state of the art research and development findings on this very broad matter through 22 original and innovative research studies exhibiting various investigation directions. The present book is a result of contributions of experts from international scientific community working in different aspects of vibration analysis. The text is addressed not only to researchers, but also to professional engineers, students and other experts in a variety of disciplines, both academic and industrial seeking to gain a better understanding of what has been done in the field recently, and what kind of open problems are in this area.

### **How to reference**

In order to correctly reference this scholarly work, feel free to copy and paste the following:

Eduardo Rubio and Juan C. Jáuregui (2011). Time-Frequency Analysis for Rotor-Rubbing Diagnosis, Advances in Vibration Analysis Research, Dr. Farzad Ebrahimi (Ed.), ISBN: 978-953-307-209-8, InTech, Available from: <http://www.intechopen.com/books/advances-in-vibration-analysis-research/time-frequency-analysis-for-rotor-rubbing-diagnosis>

**INTECH**  
open science | open minds

### **InTech Europe**

University Campus STeP Ri  
Slavka Krautzeka 83/A  
51000 Rijeka, Croatia  
Phone: +385 (51) 770 447  
Fax: +385 (51) 686 166  
[www.intechopen.com](http://www.intechopen.com)

### **InTech China**

Unit 405, Office Block, Hotel Equatorial Shanghai  
No.65, Yan An Road (West), Shanghai, 200040, China  
中国上海市延安西路65号上海国际贵都大饭店办公楼405单元  
Phone: +86-21-62489820  
Fax: +86-21-62489821



© 2011 The Author(s). Licensee IntechOpen. This chapter is distributed under the terms of the [Creative Commons Attribution-NonCommercial-ShareAlike-3.0 License](https://creativecommons.org/licenses/by-nc-sa/3.0/), which permits use, distribution and reproduction for non-commercial purposes, provided the original is properly cited and derivative works building on this content are distributed under the same license.

IntechOpen

IntechOpen